Elastic Anomalies in a Spin-Crossover System: Ferropericlase at Lower Mantle Conditions

Zhongqing Wu,[1,2,3] João F. Justo,[1,4] and Renata M. Wentzcovitch[1,5,*]

[1]Department of Chemical Engineering and Materials Science, University of Minnesota, Minneapolis, Minnesota 55455, USA
[2]Laboratory of Seismology and Physics of Earth's Interior, School of Earth and Space Sciences, University of Science and Technology of China, Hefei, Anhui 230026, China
[3]Mengcheng National Geophysical Observatory, School of Earth and Space Science, University of Science and Technology of China, Hefei, Anhui 230026, People's Republic of China
[4]Escola Politécnica, Universidade de São Paulo, CP 61548, CEP 05424-970 São Paulo, São Paulo, Brazil
[5]Minnesota Supercomputer Institute, University of Minnesota, Minneapolis, Minnesota 55455, USA

(Received 30 December 2012; published 30 May 2013)

The discovery of a pressure induced iron-related spin crossover in $Mg_{(1-x)}Fe_xO$ ferropericlase (Fp) and Mg-silicate perovskite, the major phases of Earth's lower mantle, has raised new questions about mantle properties which are of central importance to seismology. Despite extensive experimental work on the anomalous elasticity of Fp throughout the crossover, inconsistencies reported in the literature are still unexplained. Here we introduce a formulation for thermoelasticity of spin crossover systems, apply it to Fp by combining it with predictive first principles density-functional theory with on-site repulsion parameter U calculations, and contrast results with available data on samples with various iron concentrations. We explain why the shear modulus of Fp should not soften along the crossover, as observed in some experiments, predict its velocities at lower mantle conditions, and show the importance of constraining the elastic properties of minerals without extrapolations for analyses of the thermochemical state of this region.

DOI: 10.1103/PhysRevLett.110.228501 PACS numbers: 91.60.Gf, 91.60.Fe, 91.60.Lj

The elastic properties of $Mg_{1-x}Fe_xO$ ferropericlase (Fp), (Mg, Fe, Al)(Al, Fe, Si)O_3 perovskite (Pv), and postperovskite (PPv) are essential for analyses of seismic data from the lower mantle, particularly for constraining its chemical composition. Since the discovery of the high spin (HS) to low spin (LS) crossover in iron in these minerals under pressure [1,2] its effect on the elastic properties of Fp have been measured several times by various techniques [3,4]. However, the anomalies caused by the crossover have not been well reproduced across techniques. Impulsive stimulated scattering [5] showed softening in elastic coefficients C_{11}, C_{12}, and C_{44} between 40 and 60 GPa [5]. Brillouin scattering found strong softening in C_{11} and C_{12}, but not in C_{44} [6,7]. Shear velocity (V_S) measurements found an increase in V_S [8], consistent with Brillouin data [6,7]. Inelastic x-ray scattering [9] found yet different effects: softening in C_{44}, small variation in C_{12}, and no noticeable effect in C_{11}. These inconsistencies reveal a possible multitude of extrinsic effects that could have originated on, e.g., the technique, experimental conditions, sample integrity, etc. Softening of the adiabatic bulk modulus K_S has been reported by both theory [10,11] and experiments [5,7] consistent with softening of the isothermal bulk modulus K_T observed in experimental compression curves [3,12–15].

Understanding intrinsic effects of a spin crossover on elasticity requires a theoretical framework based on a minimum set of sensible assumptions [10,11,16] from which a rigorous formulation can be developed. We introduce here such formulation and elucidate the nature of intrinsic effects of spin crossovers. This formulation allows us to address the origin of some experimental discrepancies. By combining this formulation with density-functional theory with on-site repulsion parameter U(DFT + U) calculations [17] we obtain the elasticity and velocities of Fp at lower mantle conditions. DFT+U [17] is widely used and quite successful in the investigations of transition metal oxides [17]. Transition pressures are generally sensitive to the choice of exchange and correlation functional [18]. We chose the local density approximation plus on-site repulsion parameter $+U$ functional since it gives good thermal and structural properties for this class of minerals [10,11]. Although it underestimates static transition pressures [16] inclusion of vibrational effects corrects the crossover pressures to a great extent at high temperatures [10]. For iron complexes, the optimized Perdew-Burke-Ernzerhof functional is also widely used to describe their spin states [18].

At 0 GPa Fp takes on the rocksalt structure. Iron is in the HS ($S = 2$) state, but under pressure the spin state changes to LS ($S = 0$). This change occurs over a broad pressure range that increases with temperature. This is consequence of localized spin state changes that produce a mixed spin (MS) state during the crossover, with HS and LS populations determined by thermodynamic equilibrium [10,11,16]. There are significant changes in thermodynamics [11] and structural properties throughout the crossover, as seen in experimental compression curves [3,4]. The volume reduction $\Delta V^{HS\to LS}$ associated with the spin-state change enhances compression during the crossover producing the well-known bulk modulus softening [5,10]. However, the effect of the crossover on individual elastic coefficients is still not well understood [5–9].

We address this problem from a fundamental perspective. The MS state has been described as an ideal solid solution of pure HS and LS states [10,11,16]. The Gibbs free energy of this state is

$$G(n,P,T) = nG_{\rm LS}(P,T) + (1-n)G_{\rm HS}(P,T) + G_{\rm mix}, \qquad (1)$$

where $n = n(P,T)$ is the fraction of irons in the LS state, $G_{\rm LS}$ and $G_{\rm HS}$ are Gibbs free energies of pure LS and HS states, and $G_{\rm mix}$ is the ideal solid solution free energy of mixing. Elastic compliances S^{ij} are defined as

$$S^{ij} = -\frac{1}{V}\frac{\partial^2 G}{\partial\sigma_i\partial\sigma_j}\bigg|_{P,T}, \qquad (2)$$

where σ_j are stress components in Voigt notation, V is volume, and P is pressure. Elastic compliances are then given by (see Supplemental Material [19])

$$S^{ij}V = nS^{ij}_{\rm LS}V_{\rm LS} + (1-n)S^{ij}_{\rm HS}V_{\rm HS} - \left(\frac{\partial G_{\rm LS}}{\partial\sigma_j} - \frac{\partial G_{\rm HS}}{\partial\sigma_j}\right)\frac{\partial n}{\partial\sigma_i}. \qquad (3)$$

The first two terms on the right-hand side above give a weighted average of the compliances of pure HS and LS states. The third term only appears in the MS state. $[\partial n/\partial\sigma_i]$ causes the observed anomalies in K_S and K_T [10,11]. S^{11} and S^{12} should present anomalies in cubic systems since $[\partial n/\partial\sigma_1] \neq 0$. However, $n(\sigma_4)$ is an even function of σ_4 and $[\partial n/\partial\sigma_4]_{\sigma_4=0} = 0$. The elastic compliances of cubic systems then become (see Supplemental Material [19])

$$S^{11}V = nS^{11}_{\rm LS}V_{\rm LS} + (1-n)S^{11}_{\rm HS}V_{\rm HS} - \frac{1}{9}(V_{\rm LS} - V_{\rm HS})\frac{\partial n}{\partial P}, \qquad (4a)$$

$$S^{12}V = nS^{12}_{\rm LS}V_{\rm LS} + (1-n)S^{12}_{\rm HS}V_{\rm HS} - \frac{1}{9}(V_{\rm LS} - V_{\rm HS})\frac{\partial n}{\partial P}, \qquad (4b)$$

$$S^{44}V = nS^{44}_{\rm LS}V_{\rm LS} + (1-n)S^{44}_{\rm HS}V_{\rm HS}. \qquad (4c)$$

The anomalies in S^{11} and in S^{12} have equal magnitudes. $\Delta V^{\rm HS\to LS} < 0$, $\partial n/\partial p > 0$, and the last terms in Eqs. (4a) and (4b) produce anomalous increases in these compliances and softening in the corresponding elastic coefficients (see Supplemental Material [19]). This term is absent in S^{44} and in $(S^{11} - S^{12})$. Thus, C_{44} and $C' = (C_{11} - C_{12})/2$ should not soften during the spin crossover.

Adiabatic elastic coefficients of Fp with $x = 0.1875$ are compared with data in Fig. 1. Present calculations build on previously reported results [10,11] (see Supplemental Material [19]). C_{11} and C_{12} exhibit equally deep valleys that broaden and decrease in magnitude with increasing temperature. The magnitude and width of the anomaly are controlled by $\Delta V^{\rm HS\to LS}$, $\Delta G^{\rm HS\to LS}$, and temperature. $\Delta V^{\rm HS\to LS}$ in Fp with $x = 0.1875$ is $\sim -4.2\%$, which compares well with the experimental value of $\sim -3-4\%$ for $x = 0.17$ [3,12]. Our results may overestimate magnitudes and underestimate widths of elastic anomalies since calculations considered only uniform iron configurations. Inclusion of other atomic configurations would broaden the crossover pressure range [12,20,21]. Nevertheless, elastic coefficients and anomalies for $x = 0.1$ are in very good agreement with experimental data for the same composition [6] (see Supplemental Material [19]). Anomalies in C_{11} and C_{12} may reduce these coefficients by $\sim$200 GPa at 300 K. This might be slightly overestimated and the calculated C_{12} becomes slightly negative. Yet, $C' = (C_{11} - C_{12})/2$, one of Born stability criteria, remains positive. C' and C_{44} always increase with pressure, faster though during the crossover because $C^{\rm LS}_{ij} > C^{\rm HS}_{ij}$ [see Eq. (4)].

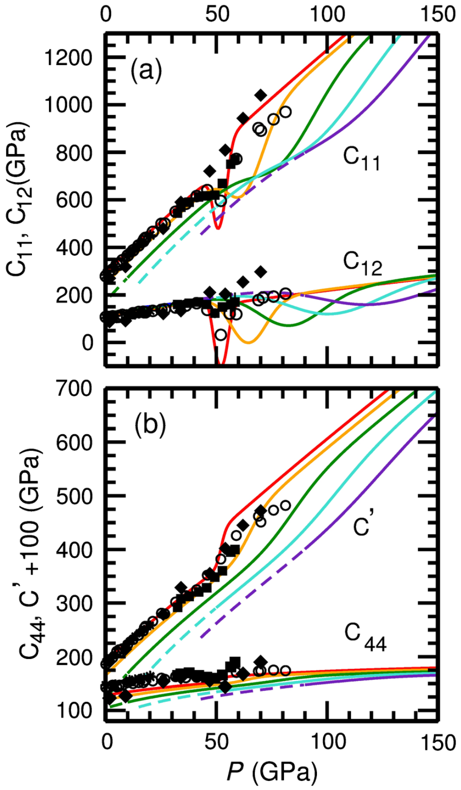

FIG. 1 (color online). Pressure dependence of thermal elastic coefficients of Fp with $x = 0.1875$ compared with experimental data at ambient temperature in samples with different x [5,6,9,29]. Full (dashed) lines represent regions inside (outside) the limit of validity of the quasi-harmonic approximation. Experimental data at ambient temperature are represented by: filled diamonds $x = 0.17$ [9], filled squares for $x = 0.06$ [5], open squares for $x = 0.06$ [29], and circles for $x = 0.10$ [6]. Color code: 300 K (red), 1000 K (orange), 2000 K (green), 3000 K (blue), and 4000 K (indigo).

Inconsistency between some experimental data sets [5,6] may be addressed in light of this analysis. The measured anomaly in C_{44} [5] may have resulted from, e.g., nonhydrostatic stresses. Deviatoric stresses should reduce symmetry more easily in Fp than in MgO because of extra internal degrees of freedom. Ferrous iron in the HS state has one minority electron in one of t_{2g} orbitals (d_{xy}, d_{yz}, or d_{zx}) and produces a localized (Jahn-Teller) distortion [16]. Macroscopic cubic symmetry suggests all three t_{2g} orbitals are equally populated throughout the sample. However, deviatoric stresses may cause preferred orbital orientation for these minority orbitals enhancing signs of symmetry reduction. Deviatoric stresses might have caused anomalous softening in C_{44} measured by impulsive stimulated scattering [5] using Ar as high pressure medium. Ar does not sustain hydrostatic pressure as well as Ne, which was used in the Brillouin scattering experiment [6]. However, the absence of anomalies in C_{11} and C_{12} measured by the inelastic x-ray scattering [9] cannot be justified by our analysis. It is not an intrinsic effect and might be related with the large wave number of x rays used in this experiment.

K_S, shear modulus (G) [22], velocities (V_ϕ, V_S, V_P), and density (ρ) of Fp with $x = 0.1875$ are shown in Fig. 2 (see Supplemental Material [19] for details). There is a substantial reduction in K_S, V_ϕ, and V_P during the spin crossover. These quantities and the elastic coefficients are fully consistent with Brillouin data [6,7]. Magnitudes of these anomalies are also consistent with differences in x. In contrast, G and V_S increase continuously during the spin crossover consistent *only* with Brillouin data [7,8]. Data for $x = 0.1$ and 0.06 are also well reproduced (see Supplemental Material [19]). Compositional effects on the elasticity of Fp throughout the lower mantle can be summarized as follows: K_S/K_T, G, and ρ for both spin states vary essentially linearly with x for $x < 0.2$, which is consistent with experimental data [23] (see also Supplemental Material [19]). K_S for pure HS and LS states increase with x: $K_S(x, P) = K_S(0, P) + b(P)x$, with $b(P) = b + b'P$, where P is pressure ($b_{\mathrm{HS}} = 73$, $b'_{\mathrm{HS}} = -0.54$, $b_{\mathrm{LS}} = 137$, and $b'_{\mathrm{LS}} = 0.08$ for $0 < P < 136$ GPa at 300 K). G for both HS and LS states decrease with x: $G(x, P) = G(0, P) + c(P)x$, with $c(P) = c + c'P$ ($c_{\mathrm{HS}} = -95$, $c'_{\mathrm{HS}} = -1.4$, and $c_{\mathrm{LS}} = -45$, $c'_{\mathrm{LS}} = -0.6$ at the same conditions). Thus, calculated $\Delta K_S^{\mathrm{HS}\rightarrow\mathrm{LS}}$ and $\Delta G^{\mathrm{HS}\rightarrow\mathrm{LS}}$ also vary approximately linearly with x in this range of x and P. The spin crossover pressure range is approximately constant for $x < 0.2$ [16,24] and the bulk modulus softening anomaly increases almost linearly for these compositions (see Supplemental Material [19], Fig. S4). Linear dependences on x are also inferred at high temperatures.

Clarification of the effect of the iron spin change on acoustic velocities of Fp is important to address a central question in geophysics [8,10,25,26]: the temperature and composition of the lower mantle. The main issue is precisely the relative abundance of Fp in this region. Recent attempts to address this question have included the effect of spin crossover in analyses of distinct mantle properties. Measurements of iron partitioning between Fp and Pv [25] suggested an increase in x in Fp from ~0.12 to ~0.17 between 28 and 40 GPa, as suggested originally [1]. The calculated density of a pyrolite aggregate with such partitioning up to 45 GPa compared well with ρ^{PREM}, the density in the preliminary reference earth model (PREM) [27]. This result suggested that pyrolite, a conjectured lower mantle rock with chemical composition similar to that of the upper mantle, is a reasonable compositional model down to ~1200 km. This implies in a chemically homogenous and well mixed mantle at least down to this depth. Another analysis [26] explored the effect of the crossover [5,7] on the longitudinal velocity gradient, dV_P/dz, where z is depth. In the lower mantle this gradient is consistent with that of a pyrolitic aggregate along an adiabatic geotherm [28] down to 1600 km depth. At greater depth, a change in thermochemical structure seems to be

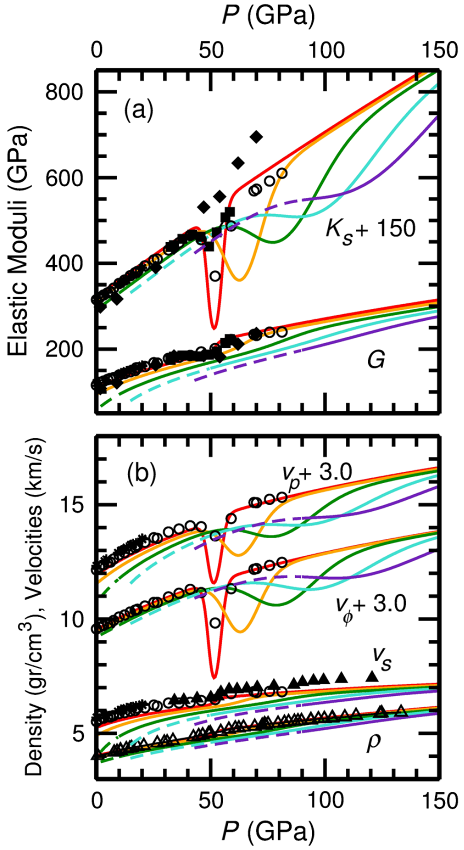

FIG. 2 (color online). Pressure dependence of (a) bulk (K_S) and shear (G) moduli and (b) compressive (V_P), shear (V_S), and bulk (V_ϕ) velocities and density (ρ) of Fp with $x = 0.1875$ compared with data in samples with different x. Experimental data are: filled diamonds for $x = 0.17$ [9], filled squares for $x = 0.06$ [5], open squares for $x = 0.06$ [29], circles for $x = 0.10$ [6], filled triangles for $x = 0.08$ [8], and open triangles for $x = 0.17$ [3]. The coloring scheme is the same one used in Fig. 1.

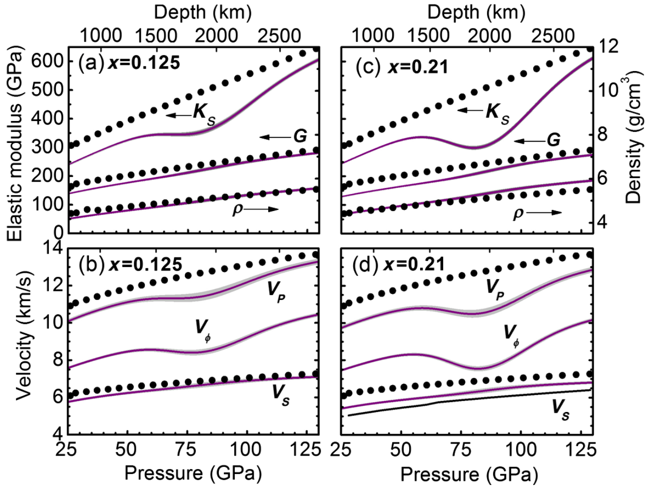

FIG. 3 (color online). (a) Elastic moduli, density, and (b) velocities of $Mg_{1-x}Fe_xO$ with $x = 0.125$ along the mantle geotherm [28]; (c) and (d) are the same for $x = 0.21$. PREM data [27] (filled circles) are shown for reference. The black line in (d) (lowest line) is the extrapolated result reported in Ref. [8] which differs by up to 9% from our predictions. Gray shaded areas are our estimated uncertainties.

required for consistency with dV_P^{PREM}/dz. Murakami's analysis of V_S in aggregates with variable amounts of Fp [8] concluded the opposite—the Mg:Si ratio in the lower mantle, starting at ~660 km depth, is more perovskitic, 1.0, than pyrolitic, 1.3, as in the upper mantle. This suggested the mantle is more chemically stratified and less-well mixed. These analyses of mantle velocities included measured effects of the spin crossover in Fp with $0.08 < x < 0.1$ at high pressures and 300 K. These measurements agree very well with our predictions (see Figs. 1 and 2 and the Supplemental Material [19]). However, extrapolations of measurements to $T > 2000$ K, of x up to 0.21, and different databases of extrapolated properties were used in these analyses. This unsettled state of affairs highlights the importance of using measurements or calculations at proper conditions and with realistic compositions, as we now present for Fp, to investigate the lower mantle thermochemical state.

Calculated aggregate elasticity and velocities of Fp along a mantle adiabat [28] for $x = 0.125$ and 0.21 are shown in Fig. 3. They are quite sensitive to x, an effect that does not appear to be well resolved experimentally in the LS state (see Figs. 1 and 2 and the Supplemental Material [19]). This may have impacted on extrapolations to different compositions and mantle temperatures [see Fig. 3(d) comparing results with extrapolations reported by Murakami *et al.* [8]]. When x increases from 0.12 to 0.21, V_P and V_S change by $\sim -4\%$ and $\sim -6\%$, respectively, in both the shallow and deep lower mantle. The anomaly in K_S changes from $\sim -6\%$ to $\sim -11\%$ at the strongest point. Therefore, a change in x with depth caused by either change in iron partitioning between Pv and Fp or by enrichment in iron with depth should affect velocities of Fp noticeably and impact on calculated mantle velocities and gradients, especially on V_P. Predicted V_S of Fp with $x = 0.21$ along the geotherm [28] are 8%–10% larger than those obtained by extrapolation of measurements in Fp with $x = 0.08$ at 300 K to $x = 0.21$ and mantle temperatures [8]. This suggests the amount of Fp in the lower mantle is larger than ~7 vol% [8], Mg:Si ratio > 1.0 and a lower mantle composition more similar to that of the upper mantle.

In summary, we have introduced a formulation for thermoelasticity of spin crossover systems and combined it with DFT + U calculations in Fp, the second major lower mantle phase. Predicted results show the importance of constraining elastic properties of minerals accurately at mantle conditions and likely compositions and of reducing uncertainties caused by extrapolations. The elasticity of Fp presented here will be a key ingredient in future analyses to the lower mantle thermochemical state, which should be based on simultaneous analyses of all seismic velocities, density, and relationships between them.

This work was supported primarily by NSF (Grants No. EAR-1047629 and No. EAR-081272) and partially supported by China-NSF (Grant No. 41274087), CAS International Partnership Program for Creative Research Teams, High-End Foreign Experts Recruitment Program of China, and FAPESP and CNPq from Brazil. Calculations were performed at the Minnesota Supercomputing Institute.

---

*wentz002@umn.edu

[1] J. Badro, G. Fiquet, F. Guyot, J. P. Rueff, V. V. Struzhkin, G. Vanko, and G. Monaco, Science **300**, 789 (2003).
[2] J. Badro, J. P. Rueff, G. Vanko, G. Monaco, G. Fiquet, and F. Guyot, Science **305**, 383 (2004).
[3] J. F. Lin, V. V. Struzhkin, S. D. Jacobsen, M. Y. Hu, P. Chow, J. Kung, H. Z. Liu, H. K. Mao, and R. J. Hemley, Nature (London) **436**, 377 (2005).
[4] J. F. Lin, G. Vanko, S. D. Jacobsen, V. Iota, V. V. Struzhkin, V. B. Prakapenka, A. Kuznetsov, and C. S. Yoo, Science **317**, 1740 (2007).
[5] J. C. Crowhurst, J. M. Brown, A. F. Goncharov, and S. D. Jacobsen, Science **319**, 451 (2008).
[6] H. Marquardt, S. Speziale, H. J. Reichmann, D. J. Frost, F. R. Schilling, and E. J. Garnero, Science **324**, 224 (2009).
[7] H. Marquardt, S. Speziale, H. J. Reichmann, D. J. Frost, and F. R. Schilling, Earth Planet. Sci. Lett. **287**, 345 (2009).
[8] M. Murakami, Y. Ohishi, N. Hirao, and K. Hirose, Nature (London) **485**, 90 (2012).
[9] D. Antonangeli, J. Siebert, C. M. Aracne, D. L. Farber, A. Bosak, M. Hoesch, M. Krisch, F. J. Ryerson, G. Fiquet, and J. Badro, Science **331**, 64 (2011).
[10] R. M. Wentzcovitch, J. F. Justo, Z. Wu, C. R. S. da Silva, D. A. Yuen, and D. Kohlstedt, Proc. Natl. Acad. Sci. U.S.A. **106**, 8447 (2009).
[11] Z. Wu, J. F. Justo, C. R. S. da Silva, S. de Gironcoli, and R. M. Wentzcovitch, Phys. Rev. B **80**, 014409 (2009).

[12] Y. W. Fei, L. Zhang, A. Corgne, H. Watson, A. Ricolleau, Y. Meng, and V. Prakapenka, Geophys. Res. Lett. **34**, L17307 (2007).

[13] K. K. Zhuravlev, J. M. Jackson, A. S. Wolf, J. K. Wicks, J. Yan, and S. M. Clark, Phys. Chem. Miner. **37**, 465 (2010).

[14] Z. Mao, J. F. Lin, J. Liu, and V. B. Prakapenka, Geophys. Res. Lett. **38**, L23308 (2011).

[15] T. Komabayashi, K. Hirose, Y. Nagaya, E. Sugimura, and Y. Ohishi, Earth Planet. Sci. Lett. **297**, 691 (2010).

[16] T. Tsuchiya, R. M. Wentzcovitch, C. R. S. da Silva, and S. de Gironcoli, Phys. Rev. Lett. **96**, 198501 (2006).

[17] M. Cococcioni and S. de Gironcoli, Phys. Rev. B **71**, 035105 (2005).

[18] M. Swart, J. Chem. Theory Comput. **4**, 2057 (2008).

[19] See Supplemental Material at http://link.aps.org/supplemental/10.1103/PhysRevLett.110.228501 for extensive details on the formalism development and comparison with experimental data on other compositions.

[20] S. Speziale, A. Milner, V. E. Lee, S. M. Clark, M. P. Pasternak, and R. Jeanloz, Proc. Natl. Acad. Sci. U.S.A. **102**, 17918 (2005).

[21] K. Persson, A. Bengtson, G. Ceder, and D. Morgan, Geophys. Res. Lett. **33**, L16306 (2006).

[22] J. P. Watt, G. F. Davies, and R. J. Oconnell, Rev. Geophys. **14**, 541 (1976).

[23] S. D. Jacobsen, H. J. Reichmann, H. A. Spetzler, S. J. Mackwell, J. R. Smyth, R. J. Angel, and C. A. McCammon, J. Geophys. Res. **107**, 2037 (2002).

[24] J. F. Lin, A. G. Gavriliuk, V. V. Struzhkin, S. D. Jacobsen, W. Sturhahn, M. Y. Hu, P. Chow, and C. S. Yoo, Phys. Rev. B **73**, 113107 (2006).

[25] T. Irifune, T. Shinmei, C. A. McCammon, N. Miyajima, D. C. Rubie, and D. J. Frost, Science **327**, 193 (2010).

[26] F. Cammarano, H. Marquardt, S. Speziale, and P. J. Tackley, Geophys. Res. Lett. **37**, L03308 (2010).

[27] A. M. Dziewonski and D. L. Anderson, Phys. Earth Planet. Inter. **25**, 297 (1981).

[28] J. M. Brown and T. J. Shankland, Geophys. J. R. Astron. Soc. **66**, 579 (1981).

[29] J. M. Jackson, S. V. Sinogeikin, S. D. Jacobsen, H. J. Reichmann, S. J. Mackwell, and J. D. Bass, J. Geophys. Res. **111**, 09203 (2006).